Ballooning Instabilities on a Magnetic Separatrix

W.X. Qu and J.D. Callen

September 1984

UWFDM-587

FUSION TECHNOLOGY INSTITUTE

UNIVERSITY OF WISCONSIN

MADISON WISCONSIN

Ballooning Instabilities on a Magnetic Separatrix

W.X. Qu and J.D. Callen

Fusion Technology Institute
University of Wisconsin
1500 Engineering Drive
Madison, WI 53706

http://fti.neep.wisc.edu

September 1984

UWFDM-587

UC-20g

BALLOONING INSTABILITIES ON A MAGNETIC SEPARATRIX

W.X. Qu[†] and J.D. Callen

Fusion Engineering Program
Nuclear Engineering Department
University of Wisconsin-Madison
Madison, Wisconsin 53706

September 1984

UWFDM-587

[†]Permanent Address: Southwestern Institute of Physics, Leshan, Sichuan, China.

I. INTRODUCTION

During high power neutral beam heating of divertor tokamak plasmas (ASDEX, D-III, PDX), the plasma can be made to change from an L-mode to an H-mode of operation, which has better energy confinement.[1] For H-mode discharges, however, edge relaxation instabilities called "H_α spikes" have been observed. Also, new quasi-coherent fluctuations (QCF) are observed.[2] The "H_α spikes" which are repetitive (~ 1 ms), short time scale bursts of light due to coolings of the plasma just inside the divertor separatrix have a drastic effect on the energy confinement.[3] In the present work, we attempt to provide an explanation for the underlying mechanism behind these edge oscillation phenomena through ballooning mode instabilities near the separatrix. One of the most important characteristics of H-mode discharges is that the plasma pressure profile in these discharges is relatively flat out to the divertor, but falls off very rapidly in the divertor separatrix region. So, in spite of the low β value near the separatrix, ballooning instabilities are still possible owing to the very large pressure gradient. To study the ballooning instabilities in the H-mode discharges, one must take account of the effect of X-points in the separatrix region, and in this paper we concentrate on the influence of the X-point on the ballooning instabilities. This work complements that by Bishop et al.[4] which examined ballooning mode stability on flux surfaces inside but approaching the separatrix.

In Section II, we derive the ballooning mode equation in a Clebsch representation. Then, in Section III, we give an analytic equilibrium configuration with two X-points at the top and bottom respectively, and obtain the explicit form of the mode equation. This is used to calculate the stability criterion for the ballooning mode in the given configuration. In Section IV,

we analyze ballooning mode instabilities in tokamak systems with concentric circular flux surfaces by using the boundary conditions derived in Section III. Section V gives a brief summary.

II. BALLOONING MODE EQUATION IN CLEBSCH REPRESENTATION

To derive the ballooning mode equation, we begin from the MHD set of equations[5]

$$\frac{\partial \rho}{\partial t} + \underline{\nabla} \cdot \rho \underline{V} = 0 \ , \tag{1}$$

$$\rho \frac{d\underline{V}}{dt} = \frac{1}{c} \underline{j} \times \underline{B} - \underline{\nabla} p \ , \tag{2}$$

$$\underline{E} + \frac{1}{c} \underline{V} \times \underline{B} = 0 \ , \tag{3}$$

$$\frac{d}{dt} (p \rho^{-\gamma}) = 0 \ , \tag{4}$$

$$\underline{\nabla} \cdot \underline{j} = 0 \ , \tag{5}$$

$$\underline{\nabla} \times \underline{B} = \frac{4\pi}{c} \underline{j} \ . \tag{6}$$

In this paper, we use the Gaussian system of units and the symbols we do not specify specifically have their usual meanings. In what follows, we use "~" on a symbol to denote a perturbed quantity and use the same symbol without "~" to denote the corresponding unperturbed quantity.

For not very large β_T, we can take

$$\tilde{\underline{E}} = -\underline{\nabla}\tilde{\phi} - \frac{1}{c}\frac{\partial \tilde{A}}{\partial t}\underline{b} \ , \tag{7}$$

$$\tilde{\underline{B}} = \underline{\nabla} \times (\tilde{A}\underline{b}) \ , \tag{8}$$

where $\underline{b} = \underline{B}/B$, and $\tilde{\phi}$ and $\tilde{A}$ are the perturbed scalar and vector potential, respectively. In a tokamak-type system, $\tilde{B}_{\parallel} \approx 0$, so the perturbed current along the field line plays a dominant role and the perpendicular perturbed current will be calculated in the electrostatic approximation.

From Eqs. (3) and (7) we have

$$\tilde{\underline{V}}_{\perp} = -\frac{c}{B^2}(\underline{B} \times \tilde{\underline{E}}_{\perp}) \ , \tag{9}$$

$$(\underline{b}\cdot\underline{\nabla})\tilde{\phi} + \frac{1}{c}\frac{\partial \tilde{A}}{\partial t} = 0 \ . \tag{10}$$

The equation for $\tilde{\phi}$ can easily be derived from

$$\underline{\nabla}\cdot\tilde{\underline{j}} = \underline{\nabla}\cdot\tilde{\underline{j}}_{\perp} + \underline{B}\cdot\underline{\nabla}\,(\tilde{j}_{\parallel}/B) = 0 \ . \tag{11}$$

It follows directly from Eqs. (2) and (3) that

$$\tilde{\underline{j}}_{\perp} = \frac{c}{B^2}\left(c\rho\frac{\partial \tilde{\underline{E}}_{\perp}}{\partial t} + \underline{B} \times \underline{\nabla}\tilde{p}\right) \ . \tag{12}$$

From Eqs. (4) and (9), we have

$$\tilde{p} = -\frac{1}{i\omega}\frac{c}{B^2}(\underline{\nabla}p \times \underline{B})\cdot\tilde{\underline{E}}_\perp \ . \tag{13}$$

In arriving at Eq. (13), the time dependence of perturbed quantities has been taken to be of the form $\exp(-i\omega t)$ and an incompressibility approximation has been made. Noting that

$$\underline{\nabla}\cdot\left(\frac{c}{B^2}\underline{B}\times\underline{\nabla}\tilde{p}\right) = -\frac{2c^2}{i\omega B^2}(\underline{b}\times\underline{\nabla}B)\cdot\underline{\nabla}(\underline{\nabla}p\times\underline{b})\cdot\tilde{\underline{E}}_\perp \ , \tag{14}$$

from Eqs. (11)-(13) we have

$$(\underline{B}\cdot\underline{\nabla})\left(\frac{\tilde{J}_\parallel}{B}\right) + \frac{c^2\rho}{B^2}(i\omega)\nabla_\perp^2\tilde{\phi} + \frac{2c^2}{i\omega B^3}(\underline{b}\times\underline{\nabla}B)\cdot\underline{\nabla}(\underline{\nabla}p\times\underline{b})\cdot\underline{\nabla}_\perp\tilde{\phi} = 0 \ , \tag{15}$$

where

$$\tilde{J}_\parallel = -\frac{c}{4\pi}\nabla_\perp^2\tilde{A} = -\frac{c^2}{4\pi i\omega}\nabla_\perp^2(\underline{b}\cdot\underline{\nabla})\tilde{\phi} \ . \tag{16}$$

If the magnetic field is given in the Clebsch representation

$$\underline{B} = \underline{\nabla}\alpha\times\underline{\nabla}\beta \ , \tag{17}$$

we have from Eq. (15) that

$$(\underline{B}\cdot\underline{\nabla})\left(\frac{\tilde{J}_\parallel}{B}\right) + \frac{c^2 i\omega\rho}{B^2}\nabla_\perp^2\tilde{\phi} - \frac{c^2}{i\omega B^2}\frac{dp}{d\alpha}\left(\frac{\partial B^2}{\partial\alpha}\frac{\partial^2\tilde{\phi}}{\partial\beta^2} - \frac{\partial B^2}{\partial\beta}\frac{\partial^2\tilde{\phi}}{\partial\alpha\partial\beta}\right) = 0 \ , \tag{18}$$

where

$$\nabla_\perp^2 = \frac{\partial}{\partial\alpha}|\underline{\nabla}\alpha|^2\frac{\partial}{\partial\alpha} + \frac{\partial}{\partial\beta}|\underline{\nabla}\beta|^2\frac{\partial}{\partial\beta} \ . \tag{19}$$

Substituting Eq. (16) into Eq. (18) yields the ballooning mode equation

$$(\underline{B}\cdot\underline{\nabla})\,\frac{1}{B^2}\,\nabla_\perp^2(\underline{B}\cdot\underline{\nabla})\tilde{\phi} + \frac{4\pi\rho\omega^2}{B^2}\,\nabla_\perp^2\tilde{\phi} + \frac{4\pi}{B^2}\,\frac{dp}{d\alpha}\left(\frac{\partial B^2}{\partial\alpha}\,\frac{\partial^2\tilde{\phi}}{\partial B^2} - \frac{\partial B^2}{\partial\beta}\,\frac{\partial^2\tilde{\phi}}{\partial\alpha\partial\beta}\right) = 0 \ . \qquad (20)$$

In the radially "local" approximation $\left(\frac{\partial\tilde{\phi}}{\partial\alpha} \,/\, \frac{\partial\tilde{\phi}}{\partial\beta} \to 0\right)$, it follows directly from Eq. (20) that

$$\left\{(\underline{B}\cdot\underline{\nabla})\,\frac{|\underline{\nabla}\beta|^2}{B^2}\,(\underline{B}\cdot\underline{\nabla}) + \frac{4\pi\rho}{B^2}\,\omega^2|\underline{\nabla}\beta|^2 + \frac{8\pi}{B}\,\frac{dp}{d\alpha}\,\frac{\partial B}{\partial\alpha}\right\}\tilde{\Phi} = 0 \ . \qquad (21)$$

In arriving at Eq. (21), we have assumed the modes to be of the form

$$\tilde{\phi} = \exp(-in\beta)\tilde{\Phi} \ . \qquad (22)$$

III. BALLOONING INSTABILITIES NEAR THE SEPARATRIX REGION FOR AN ANALYTIC EQUILIBRIUM CONFIGURATION WITH TWO X-POINTS

To facilitate the study of the influence of the divertor with two nulls on ballooning instabilities, we employ, in this section, the simple analytic equilibrium configuration shown in Fig. 1 with two X-points at the top and bottom, respectively. The magnetic field is taken to be of the form

$$\underline{B} = \frac{B_0}{1 + x/R_0}\left(\underline{e}_\zeta + \frac{x}{L_s}\,\underline{e}_y - \delta\sin\kappa y\,\underline{e}_x\right) = B_0R_0\underline{\nabla}\zeta + \underline{\nabla}\zeta\times\underline{\nabla}\psi_* \ , \qquad (23)$$

$$\psi_* = R_0B_0\left(\frac{x^2}{2L_s} - \frac{\delta}{\kappa}\cos\kappa y\right) \ , \qquad (24)$$

where ζ is the toroidal angle, R_0 is the major radius of the magnetic axis, and x and y are given in Fig. 1. From Eq. (24) we have

$$\underline{\nabla}\psi_* = R_0B_0\left(\frac{x}{L_s}\,\underline{\nabla}x + \delta\sin\kappa y\,\underline{\nabla}y\right) \ . \qquad (25)$$

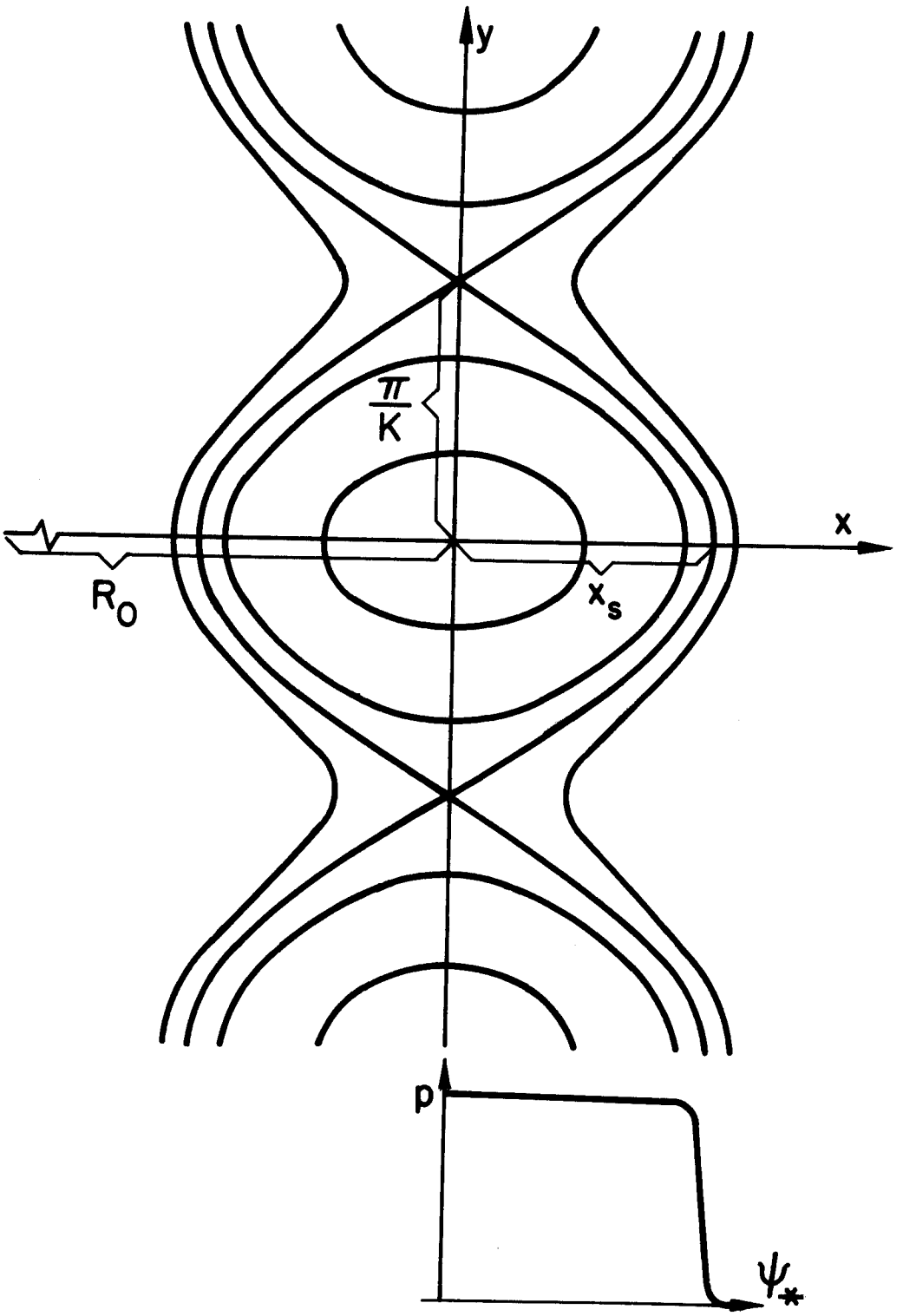

Fig. 1. An analytic equilibrium configuration with two X-points at the top and bottom, respectively. $\varepsilon_p = \pi/\kappa x_s = 1$.

The trajectory of a field line with $\psi_* =$ constant can be expressed as

$$x^2 = x_o^2 - x_s^2 \sin^2(\kappa y/2) \ , \tag{26}$$

where

$$x_s^2 = 4\delta L_s/\kappa \ , \tag{27}$$

$$x_o^2 = 2L_s\psi_*/(R_oB_o) \ . \tag{28}$$

For the separatrix, we have $x_o = x_s$,

$$x^2 = x_s^2 \cos^2(\kappa y/2) \ .$$

To express $\underline{B}$ in the Clebsch representation, we proceed as follows:

$$\begin{aligned} \underline{B} &= B_oR_o\underline{\nabla}\zeta + \underline{\nabla}\zeta \times \underline{\nabla}\psi_* = \frac{B_oR_o}{R}\,(\underline{\nabla}x \times \underline{\nabla}y) + \underline{\nabla}\zeta \times \underline{\nabla}\psi_* \\ &= \underline{\nabla}\psi_* \times (\underline{\nabla}u - \underline{\nabla}\zeta) = \underline{\nabla}\alpha \times \underline{\nabla}\beta \ , \end{aligned} \tag{29}$$

where $\alpha = \psi_* \ , \quad \beta = u - \zeta \ , \quad u = \int_o^y \frac{L_s\, dy'}{R(y',\psi_*)\, x(y',\psi_*)} \ .$ (30)

It is easy to show that in terms of the ψ_*, u, ζ coordinate system

$$\underline{B}\cdot\underline{\nabla} = \frac{R_oB_o}{R^2}\left(\frac{\partial}{\partial\zeta} + \frac{\partial}{\partial u}\right) \ , \tag{31}$$

and, hence,

$$\underline{B}\cdot\underline{\nabla}\beta = 0 \ . \tag{32}$$

Equation (32) has been used when Eq. (21) was derived. Thus, the ballooning mode equation along field lines near the separatrix is

$$\{B \frac{d}{d\ell} \alpha(\ell) B \frac{d}{d\ell} + 4\pi\rho\omega^2 \alpha(\ell) + 8\pi \frac{dp}{d\psi_*} \kappa_\alpha(\ell)\} \tilde{\Phi}(\ell) = 0 \ , \tag{33}$$

where

$$\alpha(\ell) = \frac{|\underline{\nabla}\beta|^2}{B^2} \ , \tag{34}$$

$$\kappa_\alpha(\ell) = \frac{1}{B} \frac{\partial B}{\partial \psi_*} \ . \tag{35}$$

In what follows we calculate the explicit form of Eq. (33). Setting

$$\theta = \kappa y/2 \ , \tag{36}$$

and taking the separatrix as the reference surface, we obtain

$$x = x_s \cos\theta \tag{37}$$

for the separatrix and

$$\underline{B} \cdot \underline{\nabla} = B \frac{d}{d\ell} = \frac{R_o B_o \kappa x_s}{2RL_s} \cos\theta \frac{d}{d\theta} \approx \frac{B_o \kappa x_s}{2L_s} \cos\theta \frac{d}{d\theta} \ . \tag{38}$$

From Eq. (24), we have

$$\kappa_\alpha(\ell) = - \frac{L_s}{R_o^2 B_o x_s} \frac{1}{\cos\theta} [1 + \sin\theta \cos^2\theta \, f_1(\theta)] \ , \tag{39}$$

where

$$f_1(\theta) = \int_o^\theta \frac{d\theta}{\cos^3\theta} = \frac{1}{2} [\frac{\sin\theta}{\cos^2\theta} + \ln \mathrm{tg} (\frac{\pi}{4} + \frac{\theta}{2})] \ . \tag{40}$$

Noting that

$$\frac{dp}{d\psi_*} = \frac{dp}{dx_o}\frac{dx_o}{d\psi_*} = \frac{dp}{dx_o}\frac{L_s}{R_o B_o x_s} , \tag{41}$$

the third term of Eq. (33) is then given by

$$8\pi \frac{dp}{d\psi_*}\kappa_\alpha(\ell) = -8\pi \frac{dp}{dx_o}\frac{L_s^2}{R_o^3 B_o^2 x_s^2}\frac{1}{\cos\theta}\left[1 + \sin\theta\cos^2\theta\, f_1(\theta)\right] . \tag{42}$$

From Eq. (30) we have

$$\underline{\nabla} u = \left[\frac{L_s}{R_o x_s}\frac{1}{\cos\theta} - \frac{2L_s^2\delta}{R_o x_s^3\kappa} f_1(\theta)\sin 2\theta\right]\underline{e}_y - \frac{2L_s}{R_o x_s^2\kappa} f_1(\theta)\cos\theta\,\underline{e}_x . \tag{43}$$

Since $L_s/x_s = B_o/B_a >> 1$ (B_a the poloidal magnetic field at $x = x_s$, $y = 0$), we have

$$\alpha(\ell) = \frac{1}{B^2}\left(\underline{\nabla} u - \frac{1}{R}\underline{e}_\zeta\right)^2 \approx \frac{L_s^2}{R_o^2 B_o^2 x_s^2} f_2(\theta) , \tag{44}$$

where

$$f_2(\theta) = \frac{4}{x_s^2\kappa^2}\cos^2\theta\, f_1^2(\theta) + \left[\frac{1}{\cos\theta} - \frac{1}{2}\sin 2\theta\, f_1(\theta)\right]^2 . \tag{45}$$

Substituting Eqs. (38), (42) and (44) into Eq. (33) yields the explicit form of the ballooning mode equation

$$\left\{\frac{d}{d\theta}\cos\theta\, f_2(\theta)\frac{d}{d\theta} + \frac{\omega^2}{\omega_\alpha^{*2}}\frac{1}{\cos\theta} f_2(\theta) + \frac{1}{r_p}\frac{4L_s^2\beta_T}{R_o x_s^2\kappa^2}\frac{1}{\cos^2\theta}\left[1 + \sin\theta\cos^2\theta\, f_1(\theta)\right]\right\}\tilde{\Phi}(\theta) = 0 , \tag{46}$$

where

$$r_p = -\left(\frac{1}{p}\frac{dp}{dx_o}\right)^{-1} , \qquad \beta_T = \frac{8\pi p}{B_o^2} , \qquad \omega_\alpha^{*2} = \frac{x_s^2\kappa^2 B_o^2}{16\,\pi\rho L_s^2} . \tag{47}$$

Near the X-point ($\theta \to \pi/2$), we set

$$\theta_1 = \frac{\pi}{2} - \theta \ ,$$

and Eq. (46), then, reduces to

$$\{\frac{d}{d\theta_1} \frac{1}{\theta_1} \frac{d}{d\theta_1} + \frac{\omega^2}{\omega_\alpha^{*2}} \frac{1}{\theta_1^3}\}\tilde{\Phi}(\theta_1) = 0 \ . \tag{48}$$

The finite solution to Eq. (48) is

$$\tilde{\Phi}(\theta_1) \propto \theta_1^\lambda \ , \tag{49}$$

where $$\lambda = 1 + (1 - \omega^2/\omega_\alpha^{*2})^{1/2} \approx 2 - \frac{1}{2} \frac{\omega^2}{\omega_\alpha^{*2}} \ , \qquad (\text{for } \omega^2 < \omega_\alpha^{*2}) \ . \tag{50}$$

Equation (49) can be considered as the boundary condition dictated by the X-point.

We have numerically solved Eq. (46) by the shooting method, and the results are given in Figs. 2 and 3. The variation of the critical β_T (marginally stable) with $\varepsilon_p = \pi/(x_s \kappa)$ is presented in Fig. 2. From Fig. 2 we see that the critical β_T increases with decreasing ε_p. This is because the connection length is larger for smaller ε_p. The quantities $\tilde{\Phi}$ and $\tilde{B}_\perp$ (the perturbed magnetic field perpendicular to magnetic surface) are plotted against θ in Fig. 3, and we can see that the maximum value of $\tilde{B}_\perp$ is at a point quite close to the X-point.

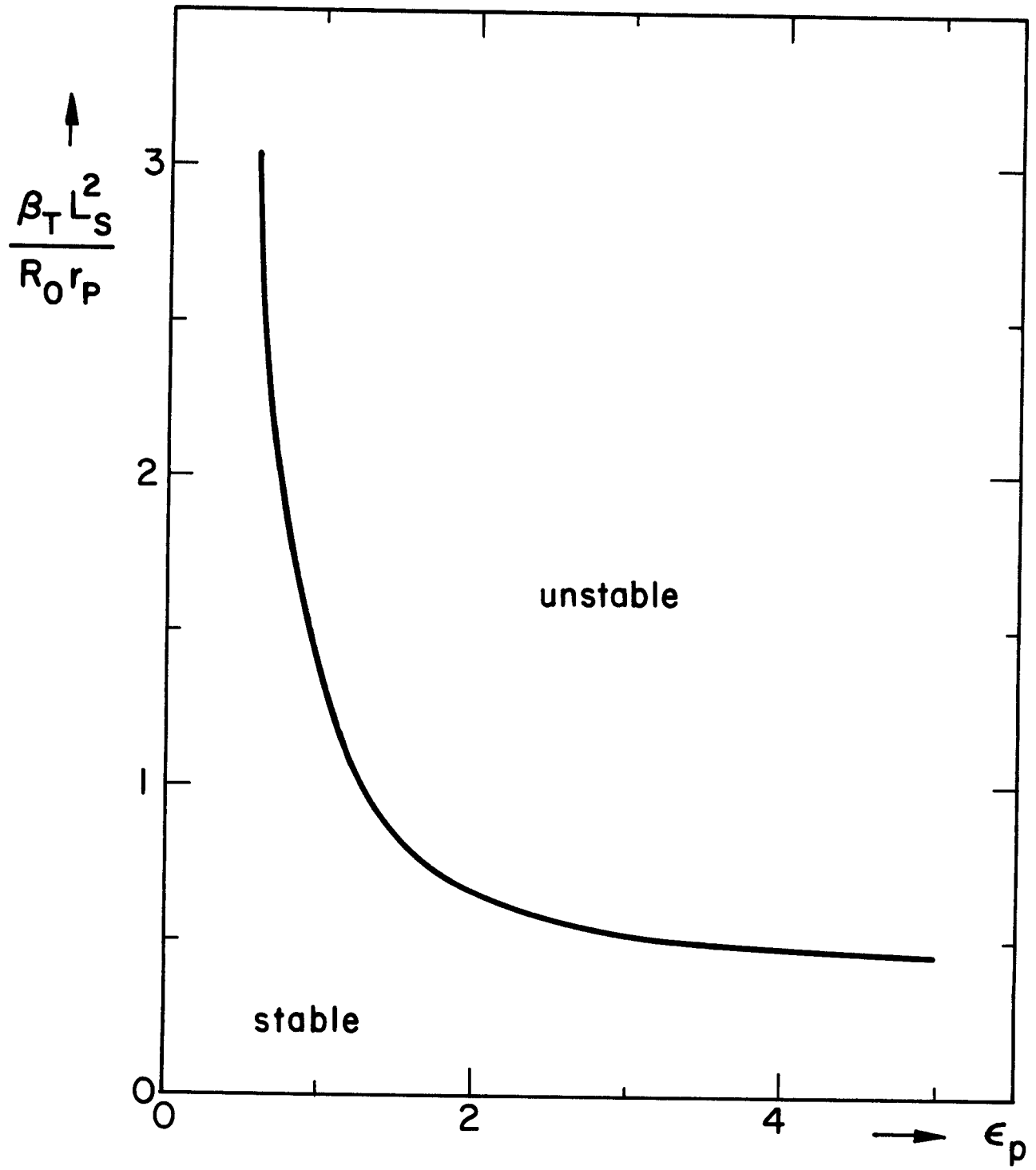

Fig. 2. The variation of critical β_T with ϵ_p.

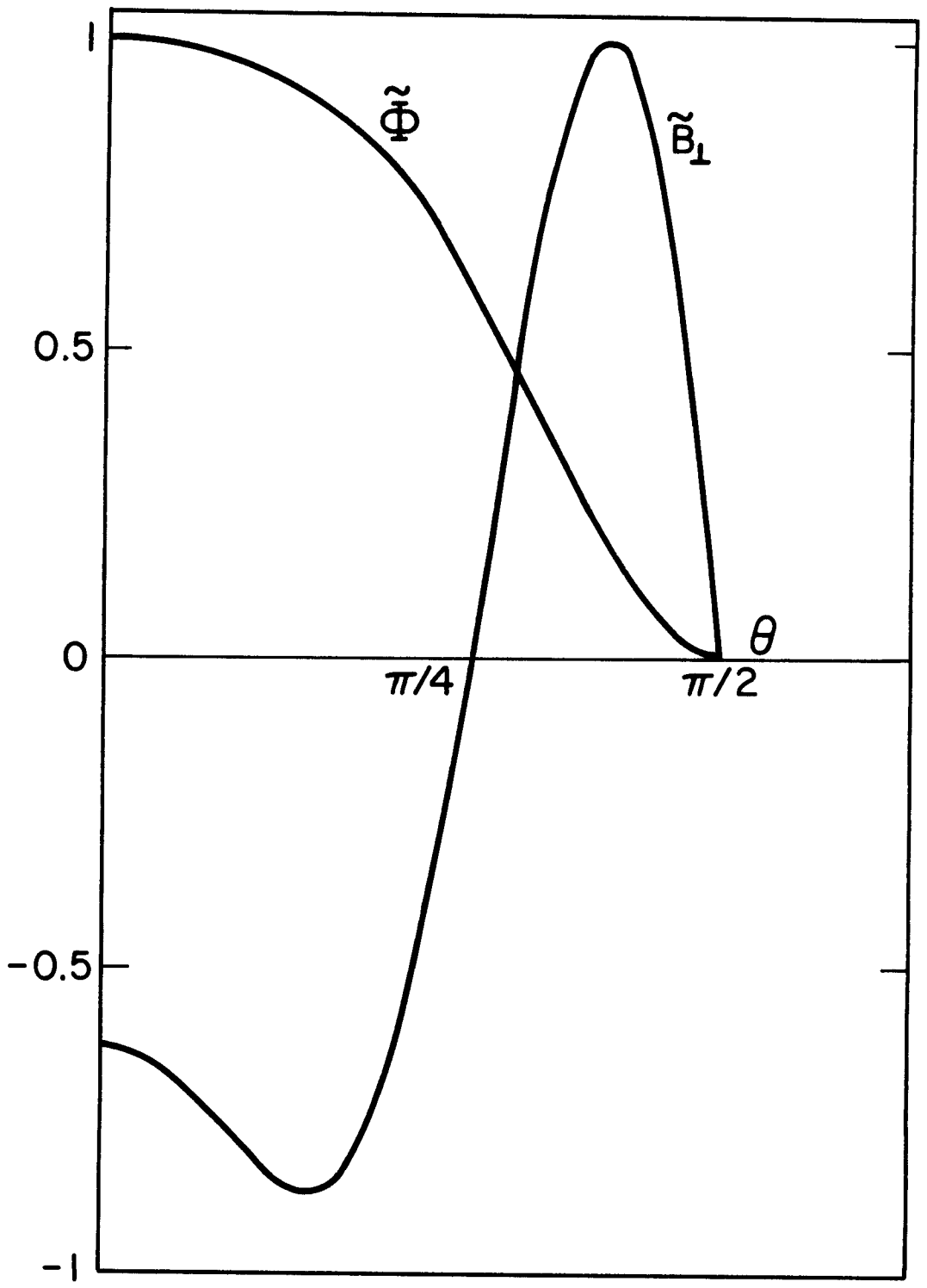

Fig. 3. The perturbed electrostatic potential $\tilde{\Phi}$ and perturbed magnetic field $\tilde{B}_\perp$ perpendicular to the magnetic surface as a function of the angular coordinate θ.

IV. BALLOONING INSTABILITIES NEAR THE SEPARATRIX FOR TOKAMAKS WITH CONCENTRIC CIRCULAR MAGNETIC SURFACES

In this section we consider ballooning instabilities in a large aspect-ratio tokamak of concentric circular magnetic surface with two divertor nulls at $(r,\theta) = (a,\pm\theta_0)$. Here we employ the coordinate system (r,θ,ζ). The X-point manifests itself through an appropriate boundary condition derived in Section III. The magnetic field is taken to be

$$\underline{B} = \frac{1}{1 + r/R_0 \cos\theta} [B_0 \underline{e}_\zeta + B_\theta(r)\underline{e}_\theta] , \tag{51}$$

or, in Clebsch representation,

$$\underline{B} = \underline{\nabla}\alpha \times \underline{\nabla}\beta , \tag{52}$$

$$\alpha = \psi = \int_0^r B_\theta(r) R_0 \, dr , \tag{53}$$

$$\beta = q\theta - \zeta . \tag{54}$$

Setting $\tilde{\phi} = \exp(-in\beta)\tilde{\Phi}$, from Eq. (20) we have

$$\{\frac{\partial}{\partial\theta} \hat{\nabla}_\perp^2 \frac{\partial}{\partial\theta} + \frac{\omega^2}{\omega_{\alpha c}^{*2}} \hat{\nabla}_\perp^2 - \frac{R_0}{r_p} \beta_T q^2 [\cos\theta - i \sin\theta(i\xi\theta - \frac{1}{k_\theta}\frac{\partial}{\partial r})]\}\tilde{\Phi} = 0 , \tag{55}$$

where

$$\beta_T = 8\pi p/B_o^2 \ , \ q = rB_o/RB_\theta \ , \ \xi = \frac{r}{q}\frac{dq}{dr} \ , \ k_\theta = nq/r \ , \ r_p = -(\frac{1}{p}\frac{dp}{dr})^{-1} \ ,$$

$$\omega^*_{\alpha c} = V_\alpha/qR_o \ , \ V_\alpha = (B_o^2/4\pi\rho)^{1/2} \ , \ \hat{\nabla}_\perp^2 = (i\xi\theta - \frac{1}{k_\theta}\frac{\partial}{\partial r})^2 - 1 \ . \qquad (56)$$

In arriving at Eq. (55), $k_\theta r = nq >> 1$ has been used.

Now we solve Eq. (55) in the following two cases.

(1) Weak Shear Approximation.

If magnetic shear is very small, we have from Eq. (56)

$$\nabla_\perp^2 = \frac{1}{k_\theta^2}\frac{\partial^2}{\partial r^2} - 1 \ , \qquad (57)$$

and Eq. (55) reduces to

$$\{(1 - \frac{1}{k_\theta^2}\frac{\partial^2}{\partial x^2})(\frac{\partial^2}{\partial\theta^2} + \frac{\omega^2}{\omega^{*2}_{\alpha c}}) + \frac{R_o}{r_p}\beta_T q^2 \ (\cos\theta + \frac{i}{k_\theta}\sin\theta\frac{\partial}{\partial x})\}\tilde{\Phi} = 0 \ , \qquad (58)$$

where $x = r - a$.

Here, in order to consider the radial structure of modes, we assume

$$\frac{1}{r_p} = \frac{1}{r_{po}}(1 - \frac{x^2}{\Delta_p^2}) \ . \qquad (59)$$

Equation (58) can be solved by separation of variables. Letting

$$\tilde{\Phi}(x,\theta) = X(x)\Theta(\theta) \ , \qquad (60)$$

and substituting Eq. (60) into Eq. (58) yields

$$\left(1 - \frac{1}{k_\theta^2}\frac{d^2}{dx^2}\right) X\left(\frac{d^2}{d\theta^2} + \frac{\omega^2}{\omega_{\alpha c}^{*2}}\right) \Theta(\theta) = -\frac{R_o}{r_p}\beta_T q^2\left(\cos\theta + \frac{i}{k_\theta}\sin\theta\,\frac{d}{dx}\right) X\Theta(\theta) \ . \qquad (61)$$

Considering even modes for $\Theta(\theta)$ and integrating Eq. (61) from $-\theta$ to θ gives

$$\frac{\left(1 - \frac{1}{k_\theta^2}\frac{d^2}{dx^2}\right) X}{\left(1 - \frac{x^2}{\Delta_p^2}\right) X} = \frac{-\frac{R_o\beta_T q^2}{r_{po}}\int_{-\theta}^{\theta}\cos\theta\ \Theta(\theta)\,d\theta}{\int_{-\theta}^{\theta}\left(\frac{d^2}{d\theta^2} + \frac{\omega^2}{\omega_{\alpha c}^{*2}}\right)\Theta(\theta)\,d\theta} = A \ , \qquad (62)$$

where A is a constant. From Eq. (62) we have

$$\left(1 - \frac{1}{k_\theta^2}\frac{d^2}{dx^2}\right) X = A\left(1 - \frac{x^2}{\Delta_p^2}\right) X \ , \qquad (63)$$

$$\left\{\frac{d^2}{d\theta^2} + \frac{\omega^2}{\omega_{\alpha c}^{*2}} + \frac{1}{A}\frac{R_o\beta_T q^2}{r_{po}}\cos\theta\right\}\Theta(\theta) = 0 \ . \qquad (64)$$

Equation (63) is easy to solve and the solution is

$$X = \exp(-\lambda x^2) \ ,$$

$$\lambda = \frac{1}{2}\left[\left(\frac{k_\theta^2}{\Delta_p^2} + \frac{1}{4\Delta_p^4}\right)^{1/2} + \frac{1}{2}\frac{1}{\Delta_p^2}\right] \ , \qquad (65)$$

$$A = \left[\frac{1}{2}\frac{1}{k_\theta\Delta_p} + \left(1 + \frac{1}{4k_\theta^2\Delta_p^2}\right)^{1/2}\right]^2 \ .$$

For $k_\theta\Delta_p \gg 1$, A takes on its minimum value, A = 1. (From Eq. (64) we can see that this case gives the most serious restriction on β_T.) Also, the perturbation is radially localized to a width of about $\Delta_p/(k_\theta\Delta_p/2)^{1/2}$, much narrower

than Δ_p. For $k_\theta \Delta_p << 1$, the perturbation is radially localized to a width of about Δ_p.

The influence of the X-point manifests itself through the boundary condition $\tilde{\Phi}$ must satisfy as θ approaches θ_o. The solution to Eq. (64) will be given later as a particular case of Eq. (67), where magnetic shear is included.

(2) Strong Shear Approximation.

If the magnetic shear is strong, we have from Eq. (56)

$$\hat{\nabla}_\perp^2 = -\xi^2\theta^2 - 1 \tag{66}$$

and Eq. (55) reduces to

$$\{\frac{d}{d\theta}(1 + \xi^2\theta^2)\frac{d}{d\theta} + \frac{\omega^2}{\omega_{\alpha c}^{*2}}(1 + \xi^2\theta^2) + \frac{R_o}{r_p}\beta_T q^2 (\cos\theta + \xi\theta \sin\theta)\}\tilde{\Phi} = 0 \ . \tag{67}$$

The boundary condition at $\theta = \theta_o$ is

$$\tilde{\Phi}(\theta) = (\theta_o - \theta)^\lambda \ ,$$
$$\lambda = 1 + (1 - \frac{\omega^2}{\omega_{\alpha c}^{*2}})^{1/2} \ , \tag{68}$$

as θ approaches θ_o. At $\theta = 0$, we have

$$\frac{d\tilde{\Phi}}{d\theta}\Big|_{\theta=0} = 0 \ , \tag{69}$$

for even modes, or

$$\tilde{\Phi}|_{\theta=0} = 0 \tag{70}$$

for odd modes. Here we consider only even modes. When $\xi = 0$, Eq. (67) reduces to Eq. (64).

The variational form of Eq. (67) is

$$\omega^2 = \frac{\int_{-\theta_o}^{\theta_o} (1 + \xi^2\theta^2) \left|\frac{d\tilde{\Phi}}{d\theta}\right|^2 d\theta - \frac{R_o\beta_T q^2}{r_p} \int_{-\theta_o}^{\theta_o} (\cos\theta + \xi\theta \sin\theta) |\tilde{\Phi}|^2 d\theta}{\frac{1}{\omega_{\alpha c}^{*2}} \int_{-\theta_o}^{\theta_o} (1 + \xi^2\theta^2) |\tilde{\Phi}|^2 d\theta} . \tag{71}$$

Taking a trial function of the form

$$\tilde{\Phi} = \cos^2\left(\frac{\pi}{2} \frac{\theta}{\theta_o}\right) , \tag{72}$$

from Eq. (71) we can get a rough estimate for the marginal stability condition. For $\theta_o = \pi/2$ (i.e., for two divertor nulls at the top and bottom) we have

$$\beta_T < \frac{15\ \pi}{32} \frac{1 + \left(\frac{\pi^2}{6} - 1\right)\xi^2}{1 + 0.2\ \xi} \frac{r_p}{q^2 R_o} , \tag{73}$$

or

$$\left|\frac{dp}{dr}\right| < \frac{15\ \pi}{32} \frac{1 + \left(\frac{\pi^2}{6} - 1\right)\xi^2}{1 + 0.2\ \xi} \frac{1}{q^2 R_o} \frac{B_o^2}{8\pi} . \tag{74}$$

Obviously, we can take $\theta_o = \pi$ to represent the usual case without divertor nulls, and the marginal stability condition in this case is

$$\beta_T < \frac{1}{2} \frac{1 + (\frac{\pi^2}{3} - \frac{1}{2})\xi^2}{1 + \frac{5}{6}\xi} \frac{r_p}{q^2 R_o} , \tag{75}$$

or

$$\left|\frac{dp}{dr}\right| < \frac{1}{2} \frac{1 + (\frac{\pi^2}{3} - \frac{1}{2})\xi^2}{1 + \frac{5}{6}\xi} \frac{1}{q^2 R_o} \frac{B_o^2}{8\pi} . \tag{76}$$

Equation (67) has been solved numerically by the shooting method and the results are given in Figs. 4 and 5. In Fig. 4, the critical β_T is plotted against magnetic shear ξ for $\theta_o = \pi/2$ and $\theta_o = \pi$. For comparison, the analytical results for critical β_T (Eqs. (73) and (75)) are given in the same figure. The electrostatic potential $\tilde{\Phi}$ is plotted in Fig. 5 for different ξ.

From Fig. 4, we can see that the X-points at the top and bottom play a stabilizing role. That is, near the separatrix the permitted pressure gradient is larger than in the usual case. However, if the pressure gradient is too large (H-mode operation may be such an example), the ballooning instabilities can still take place.

V. SUMMARY

In this work, the ballooning mode equations have been derived in a Clebsch representation and solved in two kinds of magnetic configurations that model the effects of divertor X-points. Our results show that the X-points at the top and bottom play a stabilizing role for the ballooning modes near the separatrix. Obviously, the stabilizing role comes from the reduction of the connection length because of the existence of X-points. However, if the pressure gradient near the separatrix is high enough, the ballooning instabilities can still take place. Thus, it is possible that owing to the very high pressure gradient near the separatrix, H_α spike instabilities or the quasi-

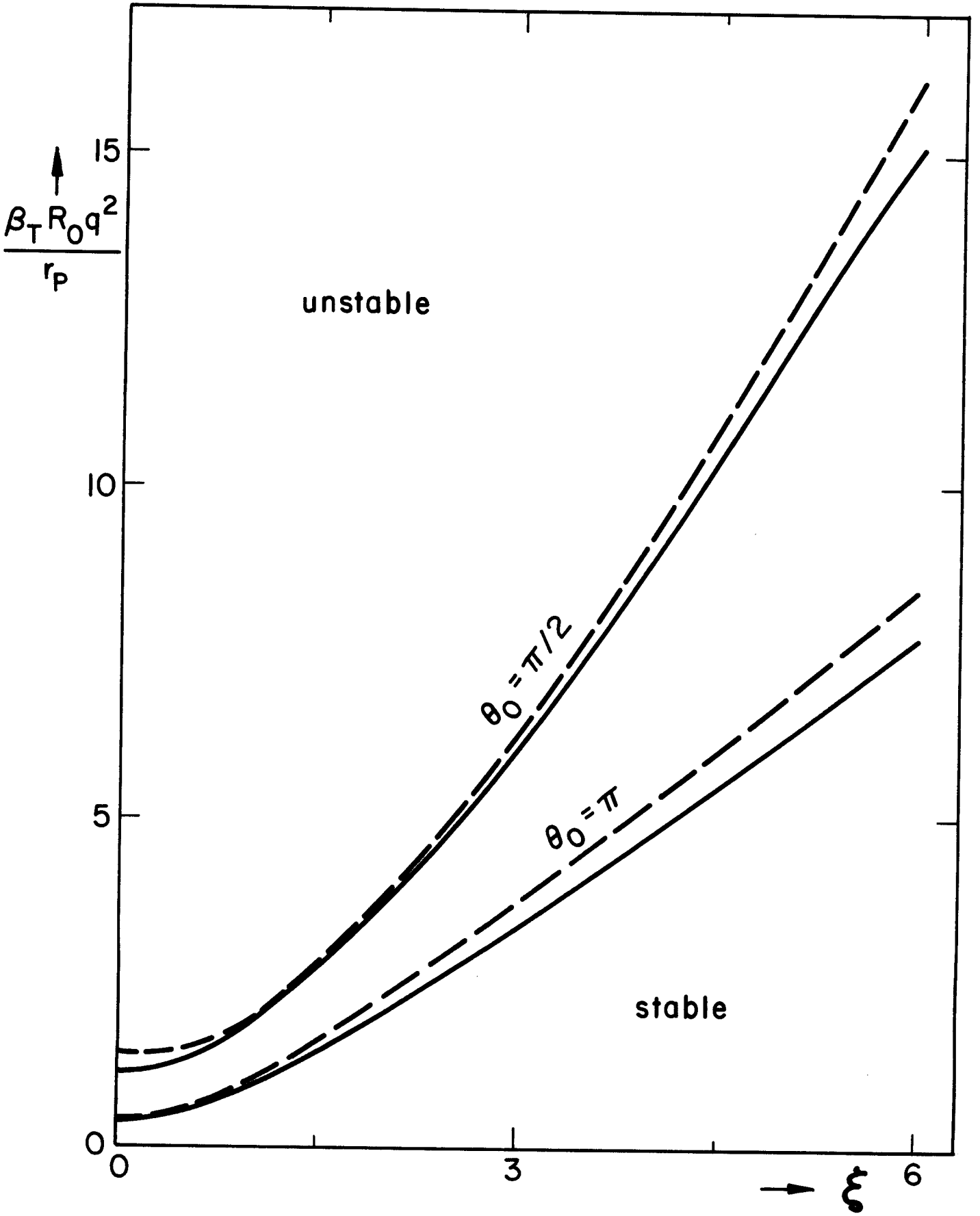

Fig. 4. The variation of critical β_T with magnetic shear ξ. The dashed lines are the analytic results and the solid lines are the numerical results.

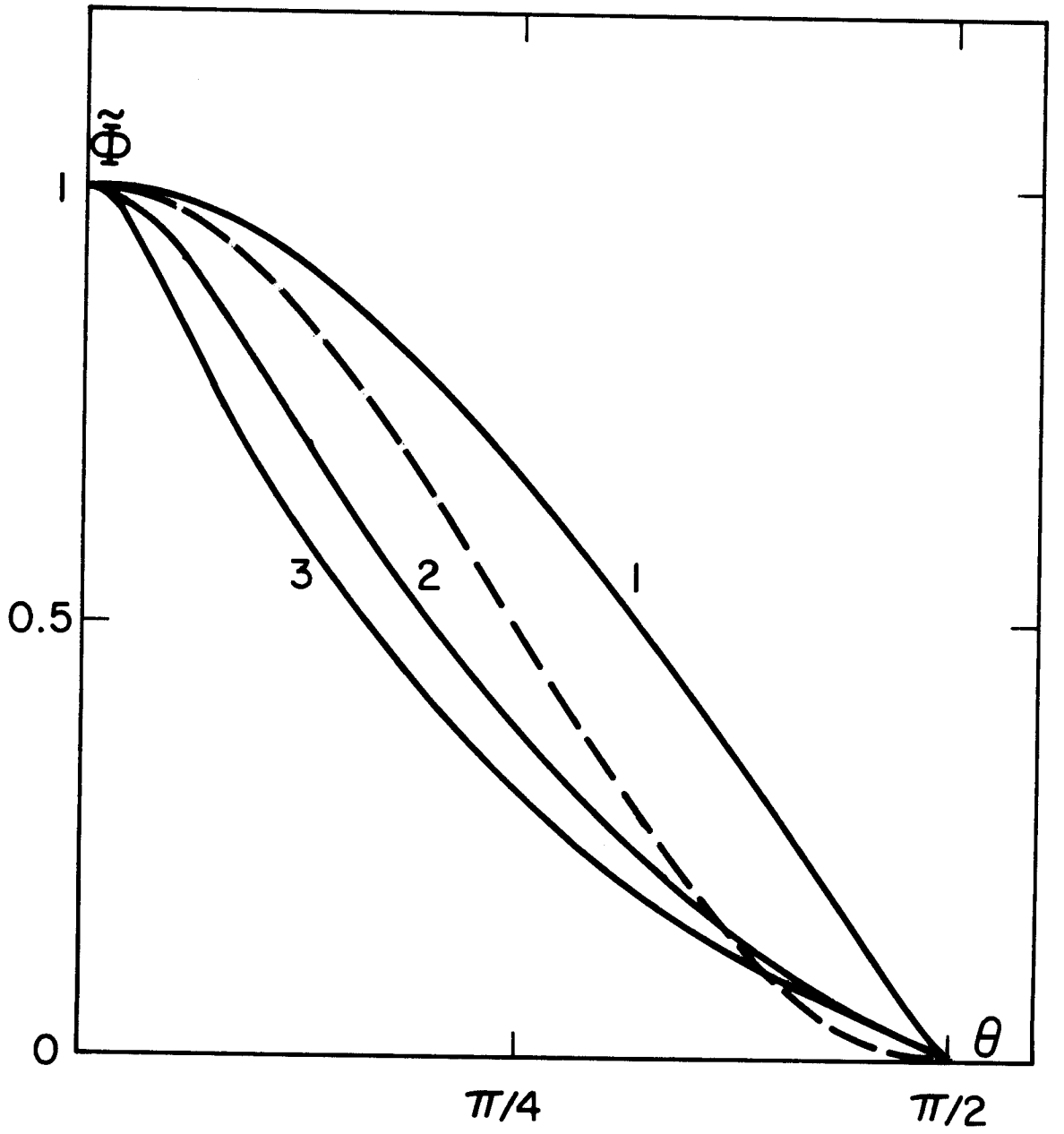

Fig. 5. The perturbed electrostatic potential $\tilde{\Phi}$ for different ξ. The curves 1, 2, 3 are for $\xi = 0, 3, 6$ respectively, and the dashed line is for the analytical trial function given by Eq. (72) with $\theta_0 = \pi/2$.

coherent fluctuations (QCF) may be caused by ballooning instabilities. The analysis here is for high mode number modes and hence most directly applicable to the quasi-coherent fluctuations; however, the same sorts of effects should also occur for the more global lower mode number modes which might play an important role in H_α spikes. Of course, to develop a more detailed understanding of the effects of these modes, the influence of the ballooning instabilities on the topological structure of the magnetic field in the X-point region should be taken into account, but that will be left for future investigation.

ACKNOWLEDGEMENTS

The authors are grateful to K. McGuire for early discussions on H-mode discharge behavior which led to the hypothesis developed in this paper. This work was supported by the U.S. Department of Energy, under contract DE-AC02-80ER53104 (JDC) and by the Southwestern Institute of Physics, Leshan, Sichuan, China (WXQ).

REFERENCES

1. F. Wagner et al., in Plasma Physics and Controlled Nuclear Fusion Research 1982 (IAEA, Vienna, 1983), Vol. I, p. 43; Phys. Rev. Letters 49, 1408 (1982).

2. R.E. Slusher et al., Phys. Rev. Letters 53, 667 (1984).

3. K. McGuire et al., in Plasma Physics and Controlled Nuclear Fusion Research 1984, (IAEA, Vienna, 1985), Vol. I, p. 117.

4. C.M. Bishop, P. Kirby, J.W. Conner, R.J. Hastie and J.B. Taylor, Nuclear Fusion 24, 1579 (1984).

5. W.A. Krall and A.W. Trivelpiece, Principles of Plasma Physics (McGraw-Hill, New York, 1973).